PAPER

The Effects of Varying Soft Handoff Thresholds in Cellular CDMA System

Bongkarn HOMNAN[†], **Watit BENJAPOLAKUL**[†a)], **Katsutoshi TSUKAMOTO**[††], ***Members***, ***and*** **Shozo KOMAKI**[††], ***Fellow***

SUMMARY In order to benefit from the advantages of soft handoff (SHO), it is important that the SHO parameters (the SHO thresholds; *T_ADD* and *T_DROP* are well assigned. *T_ADD* is the threshold used for triggering a pilot with high strength to be added to the Active Set (AS) list. The AS means the pilots associated with the forward traffic channels assigned to mobile station. In contrast, *T_DROP* is the threshold used for triggering a pilot with low strength to be dropped from the AS list. This paper analyzes the effects of varying SHO thresholds in a cellular code division multiple access (CDMA) system on the blocking probability based on traffic load and geometrical distances in hexagonal layout of base stations (BSs). In addition, the previously proposed traffic load equation [1] is applied to the proposed SHO model for balancing the numbers of new and handoff calls on the forward link capacity in case of uniform traffic load. The results show that the blocking probability is more sensitive to *T_DROP* than to *T_ADD* variations.

key words: *soft handoff, code division multiple access (CDMA), forward-link capacity, load balance equation, cell-breathing*

1. Introduction

Soft handoff (SHO) in cellular code division multiple access (CDMA) is a technique whereby a mobile station (MS) near cell boundary connects its transmitted signal to more than one base stations (BSs) within its vicinity [2], [3]. SHO is important because it provides enhanced communication quality and smoother transition compared with the conventional hard handoff. On the reverse link, the signal transmitted by an MS in the handoff area may reach all the nearby BSs, even though the signal is not intended for them and the MS signal appears as interference in these nearby cells. By putting more matched filters in the BSs receiver, BS can support more MSs in the SHO area (SHA). Notice that no extra channels are required to accomplish SHOs on the reverse links. SHO provides macro diversity, this is because more than one BSs are involved in the communications. The signal-to-interference ratio (SIR) is improved by combining the signals from different BSs, and this, in turn, increases reverse-link quality and extends cell coverage [4]. As there are at least two BSs involved in the SHO process, and each BS supports a forward-link channel to the MS, the number of available channels on the forward link decreases as the number of MSs performing SHO increases.

There are many papers that investigated the effect of SHO on system performance. Su et al. [5] analyzed system teletraffic performance in terms of blocking probability of the new and handoff calls (P_N, P_H). Kim and Sung [6] developed analytical model for SHO by introducing an overlap region between adjacent cells and the handoff call attempt rate and the channel holding times were derived. Zhang and Holtzmann [7] proposed an analysis tool for selection of the appropriate handoff thresholds based on signal strength and handoff probability. The outage probability and the number of active set updates are considered in [7]. Tcha et al. [1] derived a load balance equation from which three different loads (new call and two kinds of handoff calls) in a cell are all exactly obtained in association with the size of SHA. In those papers, only SHA was considered and the effects of varying SHO thresholds were not focused. Because *T_ADD*, the threshold used for triggering a pilot with high strength to be added to the Active Set (AS) list, and *T_DROP*, the threshold used for triggering a pilot with low strength to be dropped from the AS list, are the parameters involving with SHA, these SHO thresholds affect the system performance, such as blocking probability. Note that AS is the pilots associated with the forward traffic channels assigned to MS. Thus, in this paper, the effects of varying *T_ADD* and *T_DROP* on the blocking probability are emphasized. Moreover, the effects of cell breathing which is the effect that the cell coverage shrinks when the cell supports more users [8] are also considered in order to develop a new SHO model. Note that the load balance equation developed by Tcha et al. [1] is applied to the proposed SHO model.

2. Soft Handoff in CDMA Systems

In this paper, the term "pilot" is used to refer to the pilot channel associated with the forward CDMA channel. An MS acts as the assistant of the BS in SHO process by measuring and reporting the strength of received pilots to the BS. In performing IS-95A SHO [9], in any MS, there are channel lists, the members of which include the AS, the candidate set (CS), the neighbor set (NS) and the remaining set (RS). The AS contains the currently used channel(s). The CS contains channels, the qualities of which are almost as good as those in AS, and one of them can be chosen as a new member of AS. The NS is the set of channels which are

Manuscript received October 28, 2002.
Manuscript revised July 22, 2003.

[†]The authors are with the Department of Electrical Engineering, Faculty of Engineering, Chulalongkorn University, Phayathai Road, Bangkok 10330, Thailand.
[††]The authors are with the Department of Communications Engineering, Osaka University, Suita-shi, 565-0871 Japan.
a) E-mail: watit.b@chula.ac.th

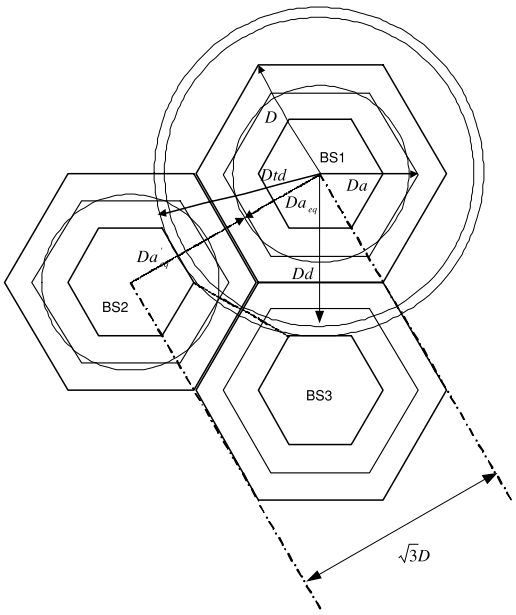

Fig. 1 Geometrical distances.

not included in the AS and CS but are reasonably strong. The RS contains the other channels that are not the members of all other sets [9], [10]. While an MS is performing SHO, it searches for the usable channels in the other cells. If the NS pilot(s) strengths are above the add threshold (T_ADD), the MS includes the pilot(s) into the CS and removes it (them) from the NS. The BS controller instructs the MS to add the new pilot(s) and the MS will add the pilot(s) to the AS, if it receives permission to add the pilot(s). If the current AS pilot(s) strength decreases below the drop threshold (T_DROP) for more than T_TDROP seconds, the MS moves the pilot(s) from the AS into the NS after it receives permission to drop the pilot(s). The AS is limited to have six pilots, while the CS is limited to five [9].

In this paper, only three pilots are used for AS. This is because at an overlap area among three cells of the proposed model as shown in Fig. 1, only strongest three pilots are considered. Besides, in this paper, the lognormal fading and Rayleigh fading are neglected for simplicity. However, the effects of these kinds of fading will be investigated in the future work.

3. The Proposed System Model

3.1 Geometrical Distances

As described in the introduction section, the previous works [5], [6], [8] considered only SHA and its effects on system performance. In fact, the SHA can be defined by some distances derived from the assigned T_ADD and T_DROP. Instead of SHA, the effects of T_ADD and T_DROP variations are emphasized in this paper. In order to show more details about the distances related to T_ADD and T_DROP, a new SHO model and the definitions of parameters in the new SHO model are described as follows. In the analytical model proposed in this paper, an MS is considered to be moving from the coverage area of BS1 to that of BS2 and there are many distances involved: the distance of cell boundary (D), the distance for adding new pilot (Da) to the AS of the outbound MS (the MS that is leaving the cell), the equivalent Da (Da_{eq}), the distance for triggering the drop timer for dropping poor pilot (Dd), and the distance for dropping poor pilot when the drop timer exceeds T_TDROP seconds (Dtd), as shown in Fig. 1. Note that the meaning of inbound MS is opposite to that of outbound MS. That is, it is defined as the MS that is entering the cell. The Da_{eq}, Dtd, and Dh, the approximated radius of handed off cell, depending on SHO thresholds and offered traffic load are proposed in this paper to develop a new SHO model. The Da_{eq} can be obtained from the assigned T_ADD and the Dtd can be obtained from the assigned T_DROP and T_TDROP.

From Fig. 1, the coverage of each cell is divided into three areas. These areas are the inner cell area (ICA), the nominal cell area (NCA) and the outer cell area (OCA). For geometrical simplicity, the ICA is bounded by the circle with a radius of Da_eq as expressed in Eq. (1) and Eq. (2)

$$ICA = \pi Da_{eq}^2 \tag{1}$$

Then,

$$Da_{eq} = \sqrt{\frac{3\sqrt{3}}{2\pi}} Da \tag{2}$$

The coverage of the NCA can be approximated by the circle with a radius of D_{eq} which can be expressed in Eq. (3)

$$Da_{eq} = \sqrt{\frac{3\sqrt{3}}{2\pi}} D \tag{3}$$

And, the OCA is approximately bounded by the ring with outer and inner radii of Dtd and Da_{eq}, respectively, as expressed in Eq. (4)

$$OCA = \pi(Dtd^2 - Da_{eq}^2) \tag{4}$$

The speed and the direction of an MS are assumed to be uniformly distributed over the intervals of [0,Vm] and [0, $1/(2\pi)$], respectively, where Vm is the maximum velocity of MS. These values remain constant for each MS when it travels. In order to investigate the effects of varying SHO thresholds, the worst case of Dtd that causes the highest blocking probability is focused and it is

$$Dtd = Dd + V_m * T\_DROP \tag{5}$$

which is the longest path [6] in the radial direction from the center of cell before an outbound MS completes its SHO process.

3.2 Distances Based on Cell Breathing-Based Pilot Signal Strength

In this paper, besides the Da_{eq}, Dtd, and Dh which are de-

pendent on SHO thresholds and offered traffic load, the effects of cell breathing are also considered in order to develop the proposed SHO model.

The attenuation (α_j) of the signal to an MS that is apart from the jth BS for r_j meters can be written [4] as

$$\alpha_j(r_j, \zeta_j) = r_j^{-\varepsilon} 10^{\zeta_j/10} \tag{6}$$

where ε is the path loss exponent and ζ is the dB attenuation due to shadowing with a zero mean and a standard deviation of σ.

The pilot signal or the ratio of the received pilot channel's chip energy to the received interference E_c/I_0 can be expressed [11] as

$$(E_c/I_0) = \frac{\beta_{P_j} P_j \alpha_j(r_j, \zeta_j)}{\sum_{k=1}^{S}\{(A_1)B\} - \beta_{P_j} P_j \alpha_j(r_j, \zeta_j) + N_{om}W} \tag{7}$$

where $A_1 = \beta_{pps_k} + \sum_{i=1}^{N_k} \gamma_{ki}\beta_{ki}$, $B = P_k\alpha_k(r_k, \zeta_k)$, P_j is the effective radiated power from the jth BS, β_{P_j} is the percentage of pilot power to the total power radiated from the jth BS, β_{ki} is the percentage of traffic channel (TCH) power to the total power, of the ith user in the kth cell, β_{pps_k} is the percentage of overhead (pilot channel, paging channel, and synchronization channel) power to the total power, of the ith user in the kth cell, S is the number of cells in the CDMA system considered in the model (only omni-directional antenna is considered in this paper), N_k is the number of users in the kth cell. γ_{ki} is the channel activity factor for TCH of the ith user in the kth cell, N_{om} is the spectral density of the ambient noise which consists of thermal noise at an MS and the other radio interferences in forward link, W is the spreaded signal bandwidth.

In the CDMA systems, the coverage boundary of forward link and SHA depend on the values of the pilot strength, T_DROP, and T_TDROP. The worst case of pilot strength normally occurs at the coverage boundary where the pilot strength the MS receives is interfered by total transmitted powers from the other BSs. Note that fast fading is assumed not to affect the average power level. It is generally assumed that the use of techniques such as interleaving, diversity, and equalization, as well as the use of RAKE receivers, greatly mitigates fast fading [12]. In addition, $N_{om}W$ is assumed to be zero [13]. Under uniform traffic load condition, $P_j = P, \beta_{P_j} = \beta_P, \beta_{ki} = \beta_i, \beta_{pps_k} = \beta_{pps}, N_k = N$, and $\gamma_{ki} = \gamma$. Therefore, from Eq. (6), Eq. (7), and Fig. 1, the distance from the jth BS for triggering the drop timer for dropping poor pilot, Dd_j can be expressed as Eq. (8).

$$10^{T\_DROP/10} = \frac{\beta_P \alpha_j(Dd_j, 0)}{\sum_{k=1}^{12}\{(A_2)\alpha_k(r_k, 0)\} - \beta_P\alpha_j(Dd_j, 0)} \tag{8}$$

where $A_2 = \beta_{pps} + \sum_{i=1}^{N} \gamma\beta_i$.

Note that ζ is assigned to be zero in order to neglect the effects of shadow fading which will be considered in the future work. The interference (the denominator) in Eq. (8) comes from 12 BSs [2], [13] as shown in Fig. 2.

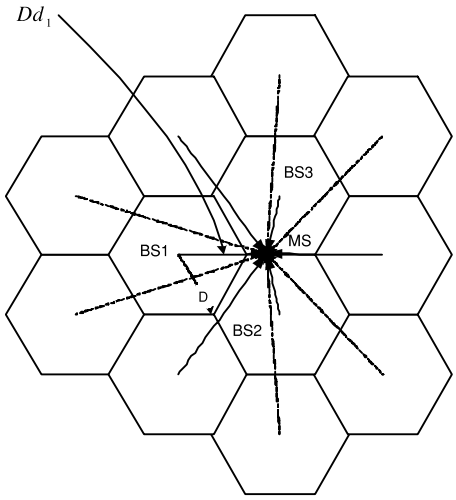

Fig. 2 Forward-link interference at an MS from 12 BSs.

It can be seen in Eq. (8) that Dd_j depends on the r_k, N, and β_i. As shown in Fig. 1, Dd_j is assumed to be equal around the cell of consideration. Thus, if an MS locates at Dd_j from the jth BS, r_k in Eq. (8) can be obtained. The relation between N and β_i, can be expressed [13] as

$$\sum_{i=1}^{N} \beta_i \le (1 - \beta_P) \tag{9}$$

In order to obtain the resultant maximum number of users (N_{max}) in each cell, Eq. (9) is approximately expressed as

$$\sum_{i=1}^{N} \beta_i = \frac{N}{N_{max}} \le (1 - \beta_P) \tag{10}$$

The N_{max} is equal to the number of Walsh codes assigned for forward link TCH (not including pilot, paging, and synchronization channels). N is the carried traffic which will be explained more in section IV. Each MS is assumed to obtain the same β_i. In fact, it is not true because the MS staying farther from the service BS should request more power than that staying near the service BS. In this paper, β_i is used as the representative value for all MSs in any BS. Thus, the closed-loop power control is assumed. In Fig. 1, Da_{eq} can be obtained as

$$Da_{eq} = \sqrt{3}D - D\acute{a}_{eq} \tag{11}$$

where $D\acute{a}_{eq}$ follows

$$10^{T\_ADD/10} = \frac{\beta_P \alpha_j(D\acute{a}_{eq}, 0)}{\sum_{k=1}^{12}\{(A_2)\alpha_k(r_k, 0)\} - \beta_P\alpha_j(D\acute{a}_{eq}, 0)} \tag{12}$$

which $A_2 = \beta_{pps} + \sum_{i=1}^{N} \gamma\beta_i$.

It can be shown that both Dd_j and in Eq. (8), Eq. (11),

and Eq. (12) are not constant and they are changed according to $\beta_P, \beta_i, \beta_{pps}$, N, γ, and r_k. D is the other parameter affecting Da_{eq}. Note that under the uniform traffic load, Dd_j, $j = 1, 2, 12$, are equal and it is represented by Dd.

4. Traffic Model

4.1 Load Balance Equation

The load balance equation was derived from the equality of traffic load imposed on the outside NCA by the calls originated in the NCA, and the load imposed inside the NCA by the active call handed off from the outside NCA at equilibrium situation [1]. The load balance equation in this paper according to the ICA, OCA, and $OCA\prime$, which is the area outside the ICA and OCA, can be expressed as

$$\begin{aligned}(C)(1-P_B) =&(\lambda_{ICA}+\lambda_{OCA})E[T](1-P_B)\\ &+\lambda_{OCA\prime}E[T]P_B\end{aligned} \tag{13}$$

where $C = \lambda_{ICA}E[T_{hICA}]+\lambda_{OCA}E[T_{hOCA}]+\lambda_{OCA\prime}E[T_{hOCA\prime}]$, P_B denotes a blocking probability of both new calls and handoff calls in any BS. It is not only a blocking probability of new calls (P_N) or not only a blocking probability of handoff calls (P_H).

The arrival processes of new calls in ICA and handoff calls from OCA are independent Poisson processes with the arrival rates of λ_{ICA} and λ_{OCA}, respectively. In addition, handoff calls enter the cell from outside according to an independent Poisson process with the arrival rate of $\lambda_{OCA\prime}$. $E[T]$ denotes the expected value of call duration time ($T = \frac{1}{\mu}$ and μ is the rate of call departures) and $E[T_{hICA}]$, $E[T_{hOCA}]$, and $E[T_{hOCA\prime}]$ denote the expected values of channel holding time for a new call originated in $ICA(T_{hICA})$, for an handoff call from $OCA(T_{hOCA})$, and for an inbound handoff call from other cells ($T_{hOCA\prime}$), respectively. Note that the $E[T_{hX}]$ can be expressed [1] as

$$\begin{aligned}E[T_{hX}] &= \int_0^\infty t[e^{-\mu t}f_{T_X}(t)+\{1-F_{T_X}(t)\}\mu e^{-\mu t}]dt\\ &= \frac{1}{\mu}-\int_0^\infty \frac{1}{\mu}e^{-\mu t}f_{T_X}(t)dt\\ &= \{1-Pr(T>T_X)\}E[T]\end{aligned} \tag{14}$$

where X can be ICA, OCA or $OCA\prime$. T_X can be T_{ICA}, T_{OCA} or $T_{OCA\prime}$. The T_{ICA} and T_{OCA} are the time periods starting from the time an MS call originates in ICA and OCA, respectively, till the time the MS finishes its SHO process to another area (OCA in case of T_{ICA} and ICA or $OCA\prime$ in case of T_{OCA}). The $T_{OCA\prime}$ is the time period starting from the time an MS call originates outside ICA and OCA of interest till the time MS comes to exist inside this ICA or OCA.

The rate of new call generations per second per NCA is denoted by λ_{NCA}. Then, λ_{ICA} and λ_{OCA} are $(ICA/NCA)\lambda_{NCA}$ and $(OCA/NCA)\lambda_{NCA}$, respectively. From [1], [14], the probability density function (pdf) of T_{ICA} related to the proposed Da_{eq} and Dtd, which are dependent on SHO thresholds, can be easily obtained as

$$f_{T_{ICA}}(t) = \begin{cases}\int_{Dtd-Da_{eq}/t}^{V_m} G\frac{1}{V_m}dw, & \text{for } M_2 \le t \le M_1\\ \int_{Dtd-Da_{eq}/t}^{Dtd+Da_{eq}/t} G\frac{1}{V_m}dw, & \text{for } M_1 \le t\end{cases} \tag{15}$$

where $G = \frac{f_1(w)}{Da_{eq}^2}$, $M_1 = \frac{Dtd+Da_{eq}}{V_m}$, $M_2 = \frac{Dtd-Da_{eq}}{V_m}$, and

$$f_1(w) = \frac{w\sqrt{-(Dtd^2-Da_{eq}^2)+2Da_{eq}^2(tw)^2-(tw)^4}}{\pi tw} \tag{16}$$

The pdf of T_{OCA} can be expressed as

$$f_{T_{OCA}}(t) = \begin{cases}\int_0^{v_m} F_2\frac{1}{V_m}dw & \text{for } 0 \le t \le M_2\\ \int_0^{v_m} F_2\frac{1}{V_m}dw - F_1 & \text{for } M_2 \le t \le M_1\\ \int_0^{v_m} F_2\frac{1}{V_m}dw - F_3 & \text{for } M_1 \le t \le \frac{(2Dtd)}{V_m}\\ \int_0^{X} F_2\frac{1}{V_m}dw - F_3 & \text{for } \frac{(2Dtd)}{V_m} \le t\end{cases} \tag{17}$$

where

$$\begin{aligned}&X = (2Dtd)/t,\\ &F_1 = \textstyle\int_{(Dtd-Da_{eq})/t}^{V_m} \frac{f_1(w)}{(Dtd)^2-(Da_{eq})^2}\frac{1}{V_m}dw,\\ &F_2 = \textstyle\frac{f_2(w)}{(Dtd)^2-(Da_{eq})^2},\\ &F_3 = \textstyle\int_{(Dtd-Da_{eq})/t}^{(Dtd+Da_{eq})/t} \frac{f_1(w)}{(Dtd)^2-(Da_{eq})^2}\frac{1}{V_m}dw, \text{ and}\\ &f_2(w) = \frac{w\sqrt{4(Dtd)^2-(tw)^2}}{\pi}\end{aligned} \tag{18}$$

The speed and direction of an incoming MS from outside the cell are denoted by v and the angle (θ) between the MS incoming direction and that pointing to the cell center from the MS position. From [1], the pdfs of the speed and direction of an incoming MS, $f_v(v)$ and $f_\theta(\theta)$ are given by

$$f_v(v) = \frac{2v}{V_m^2}, \quad \text{for} \quad 0 \le v \le V_m \tag{19}$$

$$f_\theta(\theta) = \frac{1}{2}\cos(\theta), \quad \text{for} \quad -\frac{\pi}{2} \le \theta \le \frac{\pi}{2} \tag{20}$$

Because the $f_\theta(\theta)$ gives the value of zero at the angles above $\frac{\pi}{2}$ radian (90 degree) and below $-\frac{\pi}{2}$ radian (-90 degree) as shown in Fig. 3, in addition, the $f_\theta(\theta)$ gives small value of probability at the angles close to both -90 degree and 90 degree; the area of inbound handoff calls (shaded area in Fig. 4 can be roughly approximated by the circle with a radius of Dh.

$$Dh = \frac{(Dtd + D\acute{a}_{eq})}{2} = \frac{Dtd + \sqrt{3}D - Da_{eq}}{2} \tag{21}$$

From [1], the pdf of $T_{OCA\prime}$ related to Dh can be obtained as

$$f_{T_{OCA\prime}}(t) = \begin{cases}\frac{16(Dh)^2}{3V_m^2t^3} - H & \text{for } 0 \le t \le \frac{2(Dh)}{V_m}\\ \frac{16(Dh)^2}{3V_m^2t^3} & \text{for } \frac{2(Dh)}{V_m} \le t\end{cases} \tag{22}$$

where $H = \frac{8(Dh)^2+V_m^2t^2}{3(Dh)V_mt^2}\sqrt{(\frac{2Dh}{V_mt})^2-1}$.

$E[T_{hICA}]$ and $E[T_{hOCA}]$ can be obtained from (14)–(18), and $E[T_{hOCA'}]$ can be obtained from (14) and (22). Thus, $\lambda_{OCA'}$ satisfying (13) can be obtained when the P_B is known.

4.2 Forward Link Capacity and Blocking Probability

Lee and Steele [3] investigated the capacity loss and capacity gain on the forward link. They established that the small percentage in capacity loss due to SHO (the capacity corresponding to MSs in an SHA is reduced [3] because each MS in SHA uses at least two forward-links) does not really affect the overall system capacity. However, SHO reduces the number of Walsh code channels on the forward link.

The CDMA system of interest is assumed to obey Erlang-B formula [1], [5]. Each new call is usually assigned with a channel; however, if a new call arrives when all channels are occupied, that call is lost. The offered traffic load in each cell is is $(\lambda_{ICA}+\lambda_{OCA}+\lambda_{OCA'})/\mu$; therefore, the carried traffic load (N) in Eq. (10) is approximated as $((\lambda_{ICA}+\lambda_{OCA}+\lambda_{OCA'})/\mu)(1-P_B)$. The P_B can be expressed as

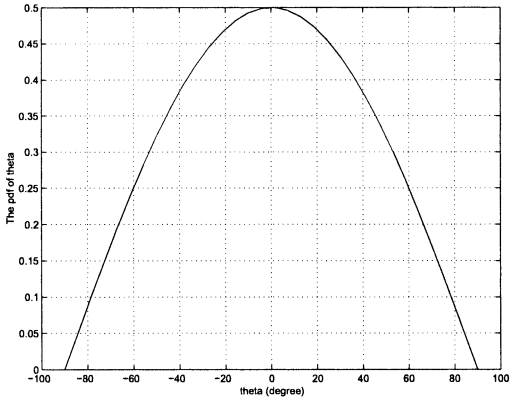

Fig. 3 The pdf of the direction of an incoming MS (pdf of theta), $f_\theta(\theta)$.

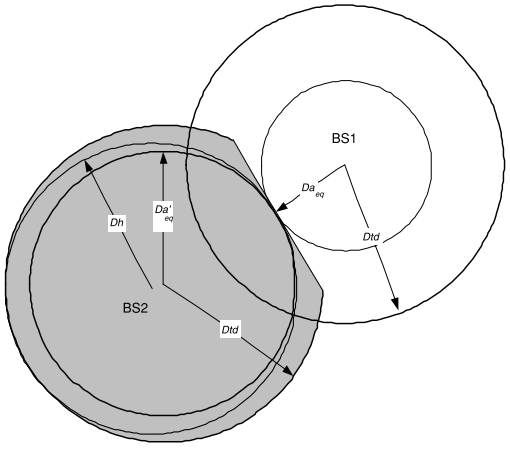

Fig. 4 Area of inbound handoff calls approximated by the circle with a radius of Dh.

$$P_B = \frac{(\lambda_{ICA}+\lambda_{OCA}+\lambda_{OCA'})^{N_{max}}}{\mu^{N_{max}}(N_{max})!}P_0 \tag{23}$$

where

$$P_0 = \frac{1}{\sum_{i=0}^{N_{max}}\frac{(\lambda_{ICA}+\lambda_{OCA}+\lambda_{OCA'})^i}{\mu^i i!}} \tag{24}$$

is the initial probability of state-transition-rate for N_{max}. The N_{max} is the number of Walsh codes assigned to the forward link TCH. Note that the relationship between P_B and both of T_ADD and T_DROP is complex and cannot be explicitly shown but this relationship can be shown graphically by using a trial error technique as described in the next section.

5. Numerical Example

The values of parameters are assigned according to [1] and [11], which are nearly the same as those used in practice, as follows: P = 5 watts, β_P = 15%, β_{pps} = 28.5%, ϵ = 4, D = 3000 m, $T = 1/\mu$ = 120 seconds, N_{max} = 50, V_m = 60 km/h, γ = 0.4, and λ_{NCA} = 0–40 (calls/hr)/km^2.

Figure 5 shows E_c/I_0 or the pilot strength of two adjacent BSs along straight line between their radii. The distance between two BSs is $\sqrt{3}D \approx$5196 m. The E_c/I_0 of each BS at higher N/N_{max} is lower than that at lower N/N_{max} because there is more interference from increased traffic loads. In other words, this phenomenon is called cell breathing. The E_c/I_0 is weaker when the MS is farther from that BS because of path loss. Normally, an MS will handoff when the E_c/I_0 of the target BS is higher than T_ADD in order to maintain the quality of the call. Thus, when the MS moves from the right side of Fig. 4 (assumed to move from the BS1's location) to the left side (BS2), the MS will handoff from the BS1 (Cell 1) to the BS2 (Cell 2) at distance Da_{eq} as shown in Fig. 6 and the MS will release TCH of the BS1 at distance Dtd as shown in Fig. 7.

The result of Da_{eq} shown in Fig. 6 can be obtained by substituting in Eq. (11) into Eq. (12). By a numerical

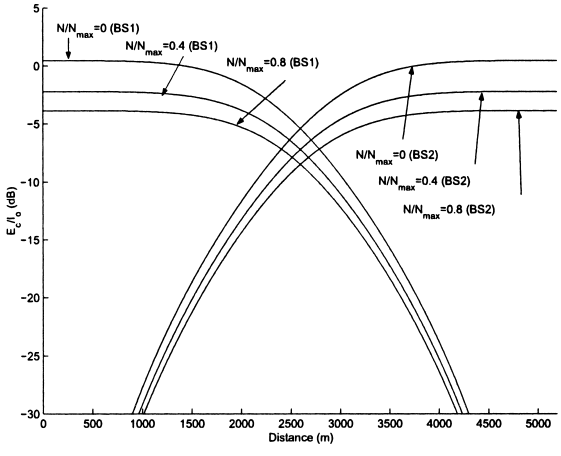

Fig. 5 $E_c/I_0(\zeta=0, T\_TDROP=0)$ as a function of distance between 2 BSs according to Eq. (7).

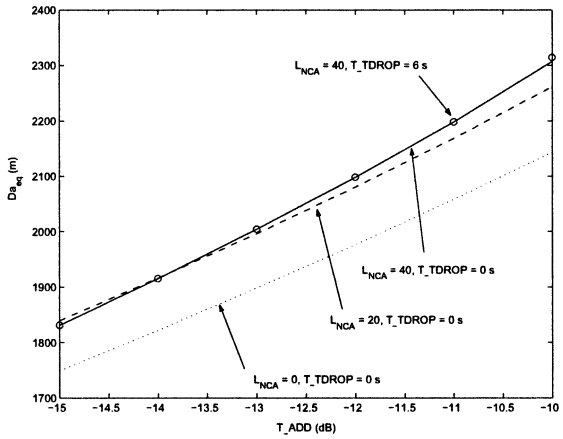

Fig. 6 Da_{eq} as a function of T_ADD according to Eq. (11) and Eq. (12), (L_{NCA}=λ_{NCA}, $T\_DROP = -15$ dB).

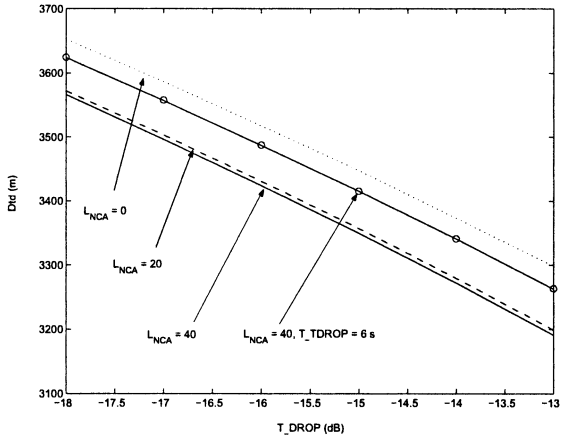

Fig. 7 *Dtd* as a function of T_DROP according to Eq. (8), (L_{NCA}=λ_{NCA}, $T\_ADD = -13$ dB).

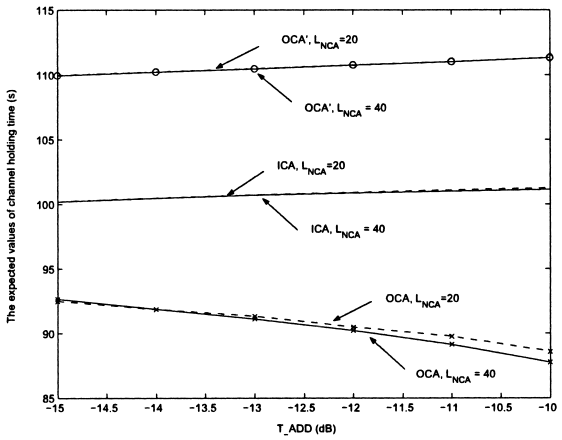

Fig. 8 The expected value of channel holding time as a function of T_ADD according to Eq. (14)–Eq. (22) with $T\_DROP = -15$ dB, (L_{NCA}=λ_{NCA}).

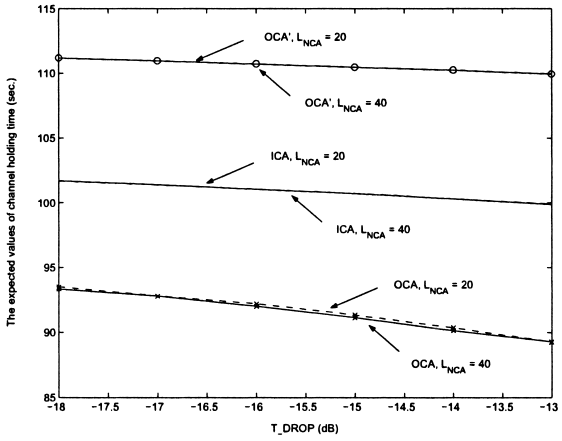

Fig. 9 The expected value of channel holding time as a function of T_DROP according to Eq. (14)–Eq. (22) with $T\_ADD = -13$ dB, (L_{NCA}=λ_{NCA}).

method, the Da_{eq} can be found. When the T_ADD of serving BS (BS1) is assigned to be lower, the MS will handoff to the BS2 at a distance closer to the BS1 as shown in Fig. 6. On the other hand, when the T_ADD of the BS1 is assigned to be higher, the MS will handoff at a farther distance from the BS1. Because there is higher interference in the cell that supports more traffic load (λ_{NCA} is high), Da_{eq} is farther from the BS1 than that in the cell that supports lower traffic load. However, the T_TDROP little affects Da_{eq} even at high traffic loads as can be observed in Fig. 6, when comparing the case of λ_{NCA}=40, T_TDROP=0 s. (solid line) to that of λ_{NCA}=40, T_TDROP=6 s. (shown by o). In contrast, because T_TDROP is the time interval for delaying the call drop of MS that is moving outbound thus the cell boundary (*Dtd*) should be affected by T_TDROP as is shown in Fig. 7, when comparing the case of λ_{NCA}=40, T_TDROP=0 s. (solid line) with that of λ_{NCA}=40, T_TDROP=6 s. (solid line with o on it).

For *Dtd*, when the T_DROP of serving BS (BS1) is assigned to be lower, the MS will release TCH of the BS1 at the distance farther from the BS1. On the other hand, when the T_DROP of the BS1 is assigned to be higher, the MS will release TCH of BS1 at a closer distance to the BS1 as shown in Fig. 7. When there is higher traffic load in a cell, the interference in that cell is higher. This makes the *Dtd* closer to the serving BS according to Eq. (8). When T_TDROP is set to be higher, MS can delay its conversation after the pilot is lower than T_DROP at least T_TDROP seconds thus the *Dtd* at higher T_TDROP is farther from the serving BS (BS1).

When T_ADD is increased, the *ICA* is increased and the *OCA* is decreased thus the expected value of channel holding time of *ICA*, $E[T_{hICA}]$, is increased and that of *OCA*, $E[T_{hOCA}]$, is decreased as shown in Fig. 8. The expected value of channel holding time of *OCA'*, $E[T_{hOCA'}]$, is increased when T_ADD is increased because the *Dh* is decreased (Fig. 4), then the $E[T_{hOCA'}]$ from Eq. (14) and Eq. (22) are increased. From Fig. 8, the expected values of all of the channel holding times at higher traffic load (40 calls/hr/km^2) are close to those at lower traffic load (20 calls/hr/km^2).

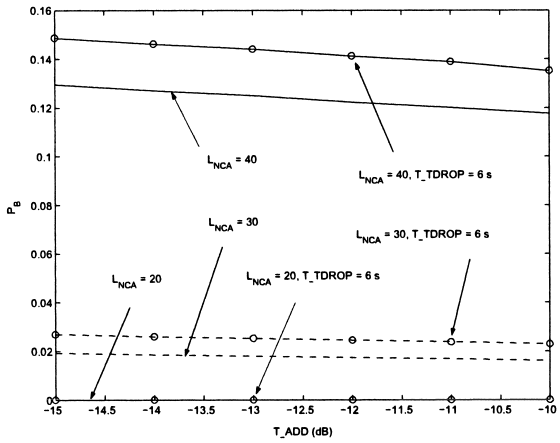

Fig. 10 P_B as a function of T_ADD with $T\_DROP = -15$ dB, (L_{NCA}=λ_{NCA}).

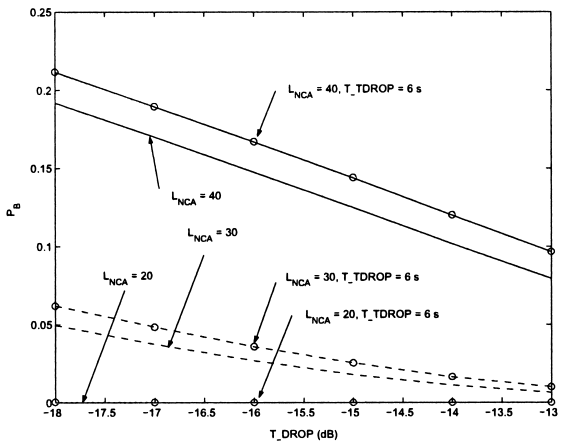

Fig. 11 P_B as a function of T_DROP with $T\_ADD = -13$ dB, (L_{NCA}=λ_{NCA}).

Figure 9 shows that when T_DROP is increased, all of channel holding times are decreased because OCA is decreased. Thus, $E[T_{hOCA}]$ is decreased. $E[T_{hICA}]$ is also decreased because, for cell with radius Dtd, there is lower probability of inbound calls coming to ICA. For inbound handoff calls, because the Dh is decreased, $E[T_{hOCA'}]$ is also decreased. In Fig. 8 and Fig. 9, the $E[T_{hOCA}]$ is the lowest when compared with the other expected values of channel holding times because it is calculated from users in OCA which is the smallest area among all of the considered areas (ICA, OCA, Circle with a radius of Dh). On the other hand, $E[T_{hOCA'}]$ is the highest when compared with those of the other expected values of channel holding times because Dh gives the highest area among all of the considered areas. Note that the expected values of all of the channel holding times at the higher traffic load (40 calls/hr/km^2) are close to those at lower traffic load (20 calls/hr/km^2).

The P_B shown in Fig. 10 can be obtained from Eq. (13), Eq. (23), and the results from Fig. 6 and Fig. 8. Figure 10 shows the P_B when T_DROP is constant at -15 dB. The P_B of higher traffic load is higher than that of lower one. At constant traffic load, when the T_ADD is set to be higher, the P_B is decreased because the percentage of calls in SHA is reduced. Note that the effect of T_ADD variation on P_B is more obvious for higher traffic load. The T_ADD does not affect P_B so much (Fig. 10) when compared with the effect of T_DROP variation (Fig. 11) because Dh of inbound handoff calls depends on Dtd (see Eq. (21)) which is obtained from T_DROP and T_TDROP and the Dtd is longer than$D\acute{a}_{eq}$.

The assigned T_ADD should not make the Da_{eq} longer than Dtd otherwise the call will be dropped before it handoffs. That is T_ADD should be set higher than T_DROP as expressed in Eq. (25).

$$T\_ADD \geq T\_DROP \tag{25}$$

The P_B shown in Fig. 11 can be obtained from Eq. (13), Eq. (23), and the results from Fig. 7 and Fig. 9. It is shown that the offered traffic load, T_DROP, and T_TDROP affect

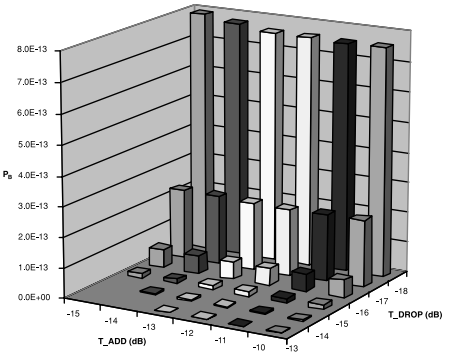

Fig. 12 P_B as a function of T_ADD and T_DROP, (λ_{NCA}=10 (cals/hr)/km^2, T_TDROP=0 sec.).

P_B. The P_B of higher traffic load or higher T_TDROP is higher than that of lower traffic load or lower T_TDROP, respectively, because the former situations have higher traffic load. Moreover, when T_DROP is increased, the P_B can be reduced very much when compared with the effect of varying T_ADD in Fig. 10; therefore the blocking probability is more sensitive to T_DROP than to T_ADD variations. The assigned T_DROP should not give Dtd shorter than Da_{eq} otherwise the call will be dropped before it handoffs according to Eq. (25). Moreover, the assigned T_DROP and T_TDROP should give the Dtd longer than D_{eq} in order to cover all of service areas. Thus the condition can be expressed as

$$Dtd(T\_DROP, T\_TDROP) > D_{eq} \tag{26}$$

where $T\_ADD \geq T\_DROP$

Figure 12–Fig. 15 show P_B as functions of both T_ADD and T_DROP at λ_{NCA} = 10–40 (calls/hr)/km^2, respectively, and T_TDROP = 0 second. There are no values of P_B at some coordinates of T_ADD and T_DROP because the constraint must be according to Eq. (26). These results show that the blocking probability is more sensitive to T_DROP than to T_ADD variations at various possible SHO thresholds according to all defined parameters in this

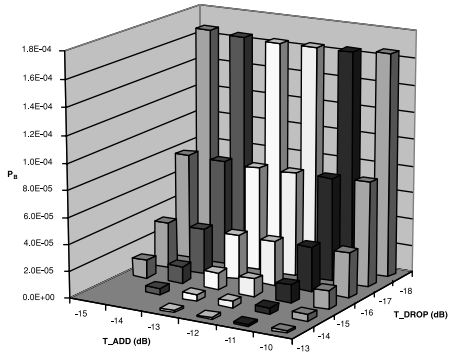

Fig. 13 P_B as a function of T_ADD and T_DROP, (λ_{NCA}=20 (cals/hr)/km^2, T_TDROP=0 sec.).

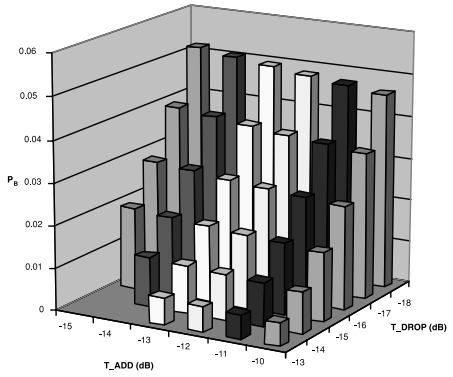

Fig. 14 P_B as a function of T_ADD and T_DROP, (λ_{NCA}=30 (cals/hr)/km^2, T_TDROP=0 sec.).

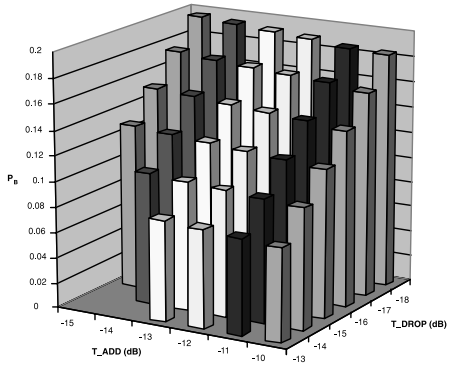

Fig. 15 P_B as a function of T_ADD and T_DROP, (λ_{NCA}=40 (cals/hr)/km^2, T_TDROP=0 sec.).

section. It is shown that at $T\_DROP = -13$ dB, the P_B is lower than those at other values of T_DROP while T_ADD at -10 dB, -11 dB, -12 dB, and -13 dB give little different P_B's. However, T_ADD at -10 dB and T_DROP at -13 dB gives the lowest value of P_B. Note that at low traffic loads ($\lambda_{NCA} < 30$) the system gives P_B with a higher degree of nonlinearity with respect to the T_ADD and T_DROP variations as shown in Fig. 12 and Fig. 13 while at high traffic loads ($\lambda_{NCA} \geq 30$), the system tends to give P_B with higher degree of linearity with respect to the T_ADD and T_DROP variations as shown in Fig. 14 and Fig. 15.

6. Conclusions

When SHO in CDMA mobile communication system is considered with the proposed SHO model on the forward link, the P_B of higher uniform traffic load or longer T_TDROP is higher than that of lower uniform traffic load or shorter T_TDROP. At any traffic load, blocking probability is more sensitive to T_DROP than to T_ADD variations. Therefore, besides the SHA, the effects of varying T_ADD and T_DROP should be considered in real system when assigning the appropriate values of SHO thresholds. The numerical example shows that the T_DROP should be set to be high and it should be selected to have Dtd longer than Da_{eq}. Moreover, the result shows that T_ADD can be assigned in wide range. In conclusion, if it is desired that P_B is effectively controlled not to be high in the forward link, instead of T_ADD, T_DROP should be adjusted.

In fact, not only blocking probability should be considered. The difference between T_ADD and T_DROP also gives different outage probability. If this is studied, the appropriate window size of these two thresholds will be known. This problem will be studied in future works. In addition, the shadowing will be considered in order to improve the proposed SHO model.

Acknowledgement

The authors wish to thank the Royal Golden Jubilee Foundation of Thailand Research Fund under grant no. PHD/0052/2542 for contribution to this research.

References

[1] D.-W. Tcha, S.-Y. Kang, and G.-W. Jin, "Load analysis of the soft handoff scheme in CDMA cellular system," IEEE J. Sel. Areas Commun., vol.19, no.6, pp.1147–1152, 2001.
[2] W.C.Y. Lee, "Overview of cellular CDMA," IEEE Trans. Veh. Technol., vol.40, no.2, pp.291–302, 1991.
[3] C.-C. Lee and R. Steele, "Effect of soft and softer handoffs on CDMA system capacity," IEEE Trans. Veh. Technol., vol.47, no.3, pp.830–841, 1998.
[4] A.J. Viterbi, A.M. Viterbi, K.S. Gilhousen, and E. Zchavi, "Soft handoff extends CDMA cell coverage and increases reverse link capacity," IEEE J. Sel. Areas Commun., vol.12, no.8, pp.1281–1288, 1994.
[5] S.-L. Su, J.-Y Chen, and J.-H. Huang, "Performance analysis of soft handoff in CDMA cellular networks," IEEE J. Sel. Areas Commun., vol.14, no.9, pp.1762–1769, 1996.
[6] D.K. Kim and D.K. Sung, "Characterization of soft handoff in CDMA system," IEEE Trans. Veh. Technol., vol.48, no.4, pp.1195–1202, 1999.
[7] N. Zhang and J.M. Holtzman, "Analysis of a CDMA soft-handoff algorithm," IEEE Trans. Veh. Technol., vol.47, no.2, pp.710–714, 1998.
[8] S.-T. Yang and A. Ephremides, "Resolving the CDMA cell breathing effect and near-far unfair access problem by bandwidth-space partitioning," IEEE 53rd Vehicular Technology Conference, pp.1037–1041, 2001.
[9] EIA/TIA/IS-95 Interim Standard, Mobile Station-Base Staion Compatibility Standard for Dual-Mode Wideband Spread Spectrum Cellular System, Telecommunication Industry Association, 1993.

[10] D. Wong and T.J. Lim, "Soft handoff in CDMA mobile systems," IEEE Pers. Commun. Mag., pp.6–17, 1997.
[11] J. Yang and W.C.Y. Lee, "Design aspects and system evaluations of IS-95 based CDMA systems," IEEE 6th Universal Personal Communications Conference Record, pp.381–385, 1997.
[12] R.P. Narrainen and F. Takawira, "Performance analysis of soft handoff in CDMA cellular networks," IEEE Trans. Veh. Technol., vol.50, no.6, pp.1507–1517, 2001.
[13] K.S. Gilhousen, I.M. Jacobs, R. Padovani, A.J. Viterbi, L.A. Weaver, and C.E. Wheatley, "On the capacity of cellular CDMA system," IEEE Trans. Veh. Technol., vol.40, no.2, pp.303–311, 1991.
[14] D. Hong and S.S. Rappaport, "Traffic model and performance analysis for cellular mobile radio telephony systems with prioritized and non-priortized handoff procedures," IEEE Trans. Veh. Technol., vol.VT-35, no.3, pp.77–92, 1986.

Bongkarn Homnan received his B.Eng., M.E., and Ph.D. in Electrical Engineering from Chulalongkorn University, Bangkok, Thailand, in 1994, 1998, and 2003, respectively. He is currently an Assistant Professor at Department of Telecommunications Engineering, Dhurakijpundit University, Thailand. His research interests include mobile communication systems and the application of artificial intelligence in communication systems. He is a member of IEEE.

Watit Benjapolakul has graduated a Doctor of Engineering degree in Electronic Engineering from University of Tokyo since 1989. He is now an Associate Professor at Department of Electrical Engineering, Chulalongkorn University, Thailand. His current research is in the field of mobile communication system, broadband network and the application of artificial intelligence in communication systems. He is currently the first Deputy Representative in the Committee for IEICE Bangkok Area Representative office.

Katsutoshi Tsukamoto was born in Shiga, Japan in October 7, 1959. He received the B.E., M.E., and Ph.D. degrees in Communications Engineering from Osaka University, in 1982, 1984, and 1995 respectively. He is currently an Associate Professor in the Department of Communications Engineering at Osaka University, engaging in the research on radio and optical communication systems. He is a member of IEEE and ITE. He was awarded the Paper Award of IEICE, Japan in 1996.

Shozo Komaki was born in Osaka, Japan, in 1947. He received B.E., M.E., and Ph.D. degrees in Electrical Communication Engineering from Osaka University, in 1970, 1972, and 1983 respectively. In 1972, he joined the NTT Radio Communication Labs., where he was engaged in repeater development for a 20-GHz digital radio system, 16-QAM and 256-QAM systems. From 1990, he moved to Osaka University, Faculty of Engineering, and engaging in the research on radio and optical communication systems. He is currently a Professor of Osaka University. Dr. Komaki is a senior member of IEEE, and a member of the Institute of Television Engineers of Japan (ITE). He was awarded the Paper Award and the Achievement Award of IEICE, Japan in 1977 and 1994 respectively.